

RESEARCH ARTICLE

Cryptic surface-associated multicellularity emerges through cell adhesion and its regulation

Jordi van Gestel^{1,2*}, Andreas Wagner^{1,2,3*}

1 Department of Evolutionary Biology and Environmental Studies, University of Zürich, Zürich, Switzerland, **2** Swiss Institute of Bioinformatics, Lausanne, Switzerland, **3** The Santa Fe Institute, Santa Fe, New Mexico, United States of America

✉ Current address: Department of Microbiology and Immunology, University of California San Francisco, San Francisco, United States of America

* jordivangestel@gmail.com (JvG); andreas.wagner@ieu.uzh.ch (AW)

**OPEN ACCESS**

Citation: van Gestel J, Wagner A (2021) Cryptic surface-associated multicellularity emerges through cell adhesion and its regulation. *PLoS Biol* 19(5): e3001250. <https://doi.org/10.1371/journal.pbio.3001250>

Academic Editor: Nick H. Barton, Institute of Science and Technology Austria (IST Austria), AUSTRIA

Received: January 10, 2021

Accepted: April 28, 2021

Published: May 13, 2021

Copyright: © 2021 van Gestel, Wagner. This is an open access article distributed under the terms of the [Creative Commons Attribution License](https://creativecommons.org/licenses/by/4.0/), which permits unrestricted use, distribution, and reproduction in any medium, provided the original author and source are credited.

Data Availability Statement: All relevant data are within the paper, its [Supporting information files](#) and the Github repository <https://github.com/jordivangestel/PLoS-Biology-2021>.

Funding: JvG received support from the Wierenga Rengerink PhD Prize from the University of Groningen, the Marie Skłodowska-Curie Individual Fellowship (742235) and a Swiss National Science Foundation Postdoc.Mobility Fellowship (P400PB_186789). AW was supported by ERC Advanced Grant 739874, by Swiss National

Abstract

The repeated evolution of multicellularity led to a wide diversity of organisms, many of which are sessile, including land plants, many fungi, and colonial animals. Sessile organisms adhere to a surface for most of their lives, where they grow and compete for space. Despite the prevalence of surface-associated multicellularity, little is known about its evolutionary origin. Here, we introduce a novel theoretical approach, based on spatial lineage tracking of cells, to study this origin. We show that multicellularity can rapidly evolve from two widespread cellular properties: cell adhesion and the regulatory control of adhesion. By evolving adhesion, cells attach to a surface, where they spontaneously give rise to primitive cell collectives that differ in size, life span, and mode of propagation. Selection in favor of large collectives increases the fraction of adhesive cells until a surface becomes fully occupied. Through kin recognition, collectives then evolve a central-peripheral polarity in cell adhesion that supports a division of labor between cells and profoundly impacts growth. Despite this spatial organization, nascent collectives remain cryptic, lack well-defined boundaries, and would require experimental lineage tracking technologies for their identification. Our results suggest that cryptic multicellularity could readily evolve and originate well before multicellular individuals become morphologically evident.

Introduction

Surface-associated organisms can be found throughout the biosphere [1–3]. By adhering to surfaces, organisms can obtain primary access to resources important for growth. Lichens, for instance, adhere to rocks to obtain access to sunlight, and microbes colonize our teeth to consume sugars (Fig 1a). In competition for space, organisms evolved suites of multicellular adaptations that promote surface growth or dispersal, like filamentous growth, sporangia, and fruiting bodies. This raises the question how surface-associated multicellularity comes about in evolutionary time. One important challenge in studying surface-associated organisms

Science Foundation grant 31003A_172887, as well as by the University Priority Research Program in Evolutionary Biology at the University of Zurich. The funders had no role in study design, data collection and analysis, decision to publish, or preparation of the manuscript.

Competing interests: The authors have declared that no competing interests exist.

resides in their remarkable plasticity [4–7]: On a surface, organisms often display continuous growth, can merge, and adopt many different forms. This plasticity makes it difficult to apply standard evolutionary theory, like multilevel selection theory [8–10] or kin selection theory [11,12], to study how surface-associated multicellularity originates [13]. Here, we overcome this challenge by introducing a novel bottom-up approach, based on spatial lineage tracking of cells, to study how primitive cell collectives can first emerge on a surface and subsequently evolve multicellular adaptations.

The life cycle of surface-associated organisms involves both surface growth and reproduction. Surface growth relies on adhesion. Organisms express a wide variety of adhesive molecules, from extracellular polysaccharides secreted into the environment [14–17] to membrane-bound proteins that mediate cell-to-cell contact [18,19]. These molecules ensure that cells remain attached while dividing. Within a multicellular collective, cells often express diverse adhesive properties and thereby affect the spatial organization of the collective [20,21]. For example, in the soil bacterium *Bacillus subtilis*, cells differentiate into adhesive and nonadhesive cells that together promote colony expansion [21,22]. To bring about collective organization, cells can also directly interact with each other using so-called kin recognition systems, such as strain-specific cell–cell communication [23–25]. These systems generally promote cooperation between cells and thereby foster the emergence of collectivity [26]. For instance, in many surface-associated pathogens, cells employ cell-to-cell communication to collectively produce virulence factors, which are costly to express but promote infectious growth [27].

Besides growth, reproduction forms another major component in the life cycle of surface-associated organisms. A multicellular collective reproduces whenever cells disassociate from

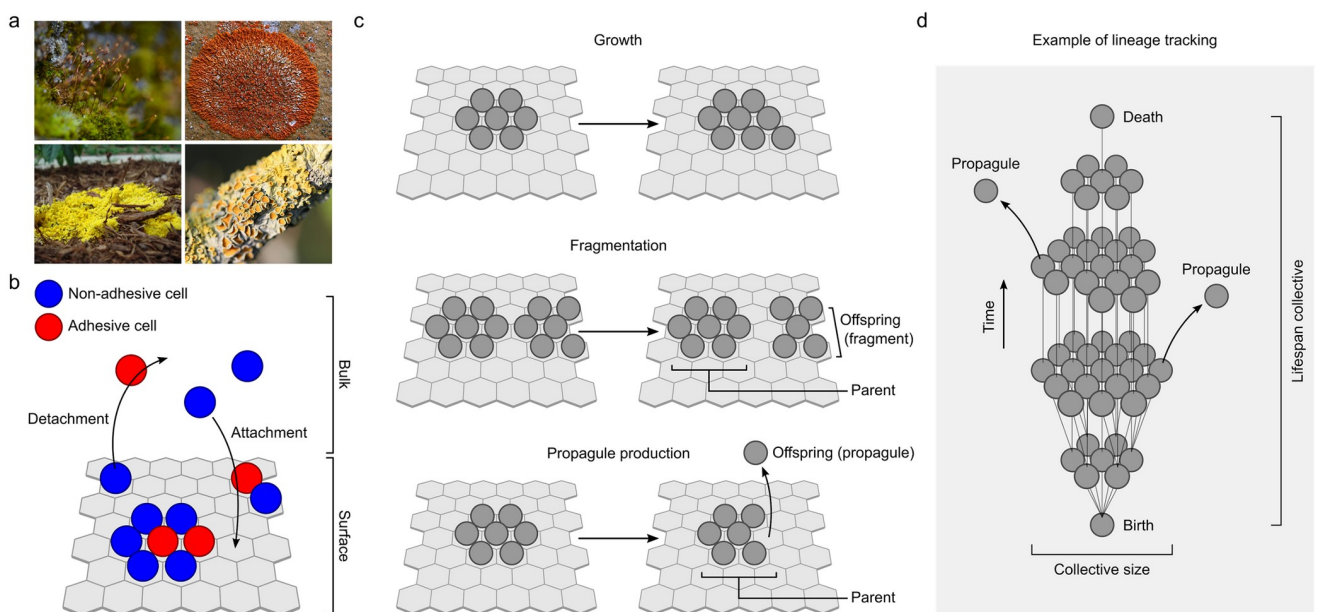


Fig 1. Surface colonization and tracking cell collectives. (a) Examples of surface-associated multicellularity, top–bottom: Bryophyta, Ascomycota, slime mold, and lichen (images are shown under the Creative Commons license from Wikimedia and Needpix; Rostislav Kralik, Jason Hollinger). (b) Schematic depiction of model adopted from [41]. Cells can occupy 2 environments: the surface and the bulk. In the bulk, cells freely move around. The surface is represented by a hexagonal grid to which cells can attach. Adhesive cells (red) can adhere to the surface independently. Nonadhesive cells (blue) can only adhere when neighboring an adhesive cell. (c) Processes of collective growth and collective reproduction. Collective reproduction can either result from fragmentation of the collective on the surface or from propagule production, where a cell detaches to the bulk. (d) Simplified depiction of lineage tracking from “birth” to “death” of a collective. Collective size is determined by the number of cells in the collective. Collective life span is determined by the number of time steps during which the collective exists.

<https://doi.org/10.1371/journal.pbio.3001250.g001>

the existing collective, with the potential of reestablishing a collective somewhere else. Collective reproduction therefore differs from cell division, as it concerns propagation of the collective and not that of the individual cell. In contrast to surface growth, which relies on adhesion, collective reproduction depends on a loss of adhesion and can take several forms [28,29]. For example, when adhesion weakens, individual cells can disassociate from the collective one by one, disperse, and colonize new surfaces. Such cells are typically referred to as propagules. By regulating adhesion, organisms can control the rate of propagule production [30–32]. For example, inside bacterial biofilms, cells can facilitate dispersal by down-regulating polysaccharide production or actively secreting enzymes that degrade polysaccharides [33,34]. Collectives can also break apart into multiple smaller collectives through a process called fragmentation [35]. In many species, including fungi, myxobacteria, and slime molds, reproduction occurs through the formation of specialized dispersal organs, called fruiting bodies, in which cells collectively rise from the surface to facilitate spore dispersal [36–38].

A critical step in understanding the emergence and subsequent evolution of multicellularity lies in understanding how changes in cell properties affect collective processes like growth and reproduction. What collective phenotypes emerge spontaneously and what other phenotypes are attainable through mutations? To address these questions from a theoretical perspective, one needs a bottom-up approach that explicitly accounts for cell properties and examines how, through the evolution of those properties, collectives emerge and evolve [31,39,40]. This approach is blind to the exact form of multicellularity that may eventually arise but instead aims at understanding the causal processes that lead to multicellular organization. Here, we model the evolution of surface colonization using such a bottom-up approach and thereby study the earliest emergence of surface-associated multicellularity [41].

Our model emulates an ecology where cells can occupy two possible environments: a surface or the bulk—the three-dimensional space above the surface (Fig 1b). For simplicity, the surface is represented by a two-dimensional hexagonal grid, where each cell can have up to 6 neighbors (see S1 Text for a discussion on alternative surface geometries). Surface attachment requires adhesion. Since adhesion is known to also mediate cell–cell contact [20,42,43], we assume that, for attachment, cells must either be adhesive themselves or associate with an adhesive cell on the surface. Thus, adhesive cells can support the attachment of nonadhesive neighbors. Detachment results from a loss of adhesion. It requires that both the detaching cell and its neighbors are nonadhesive.

In the bulk, cells do not adhere to each other and strongly compete. That is, we assume that cells in the bulk can only divide when the population size is below a given carrying capacity. Cells can escape this competition by attaching to the surface, where they can divide whenever there is space in one of the neighboring grid elements (see Methods). In other words, the surface forms a distinct ecological niche, where cells only compete for space with other surface-associated cells and not with cells from the bulk. After cell division on the surface, a daughter cell can have two possible fates: It can either remain attached to the surface through adhesion, or it can detach to the bulk (for details, see S1 Text). In many surface colonizers, adhesion requires the expression of costly molecules [42,44,45], and we thus assume that adhesion lowers the rate of cell division. When competition for space on the surface increases, because more cells attach to the surface, the costs of adhesion can outweigh its benefits (i.e., the opportunity to divide on the surface). We start by assuming that adhesion is expressed stochastically, as observed in several colony-forming bacteria [46,47].

In order to keep track of collectives that emerge on the surface, we follow their constituent cells in time [48–50], akin to methods of lineage tracking employed in both developmental biology [51] and microbiology [52] (Fig 1c and 1d). We monitor instances of (i) cell division; (ii) cell death; (iii) surface attachment; (iv) surface detachment; and (v) changes in cell

adhesion (S2 Text, S1 and S2 Figs). A surface-associated collective is seeded when a cell attaches to the surface. On the surface, this collective can grow (Fig 1c). Every time a cell divides, and its daughter cell remains attached to the surface, the collective grows by one cell. A collective reproduces when its constituent cells get disconnected, either through fragmentation or propagule production (Fig 1c). During fragmentation, formerly connected cells on the surface get disconnected because a constituent cell dies or detaches. We define the largest fragment as the parental collective and the other fragment(s) as its offspring. Propagule production occurs when single cells detach from the surface. This could either result from a loss of adhesion or from cell division (when the daughter cell detaches). Finally, we assume that cells experience a constant death rate. This implies that collectives can also die and that large collectives are less likely to die than small collectives. By tracking how a collective grows, reproduces, and dies, we can reconstruct its genealogy (S2 Fig). This allows us to examine various collective properties (Fig 1d), including spatial organization, number of offspring, and life span.

Importantly, to make sure that we account for all cells when reconstructing collective genealogies, we also consider “collectives” consisting of single cells only. For example, if a collective produces a propagule, through the detachment of a single cell from the surface, this single cell is counted as an independent collective. This implies that all cells in the bulk are traced as single cell “collectives.” Also, when collectives happen to merge on the surface, as is frequently observed in primitive surface colonizers, we still trace their constituent cells separately, so that we can monitor each collective from the first cell that seeds the collective to the last cell that dies.

Results

Surface colonization

We start our analysis by examining how the probability (P) of adhesion affects the organization of cells on the surface. As expected, the number of cells adhering to the surface increases with the adhesion probability (Fig 2a and 2b; see also S1–S10 Movies and S2 Fig). When $P > 0.35$, the surface becomes fully occupied.

On the surface, cell division can either lead to collective growth when a daughter cell remains attached, or to reproduction, when the daughter cell detaches and thus forms a propagule of the collective (S1 Fig). To determine how cell division contributes to collective reproduction, we monitor all instances of both cell division and collective reproduction on the surface. Irrespective of adhesion probability, we find that most cell division events lead to surface growth (Fig 2c). Propagule production only occurs at low and high adhesion probabilities. Specifically, when the adhesion probability is low ($P < 0.2$), cell division often leads to propagule production because newly dividing cells are likely to detach. The reason is that adhesive cells to which they could remain attached are scarce on the surface. Conversely, when the adhesion probability is high ($P > 0.35$), cell division often leads to propagule production due to a lack of space on the surface. At intermediate adhesion probabilities ($0.2 < P < 0.35$), division exclusively contributes to collective growth (Fig 2c). In this regime, collectives reproduce either through fragmentation or through propagules that detach due to a loss of adhesion. Thus, depending on the propensity to adhere, collectives display different modes of reproduction to which cell division contributes either directly or indirectly, via growth.

Next, we trace collectives from birth till death (Fig 1d, S2 Fig). This allows us to determine a collective's lifetime reproductive success, which is the total number of offspring it produces during its lifetime (S2 Fig). When the overall population size reaches equilibrium, the average lifetime reproductive success of collectives is expected to be approximately one, meaning that

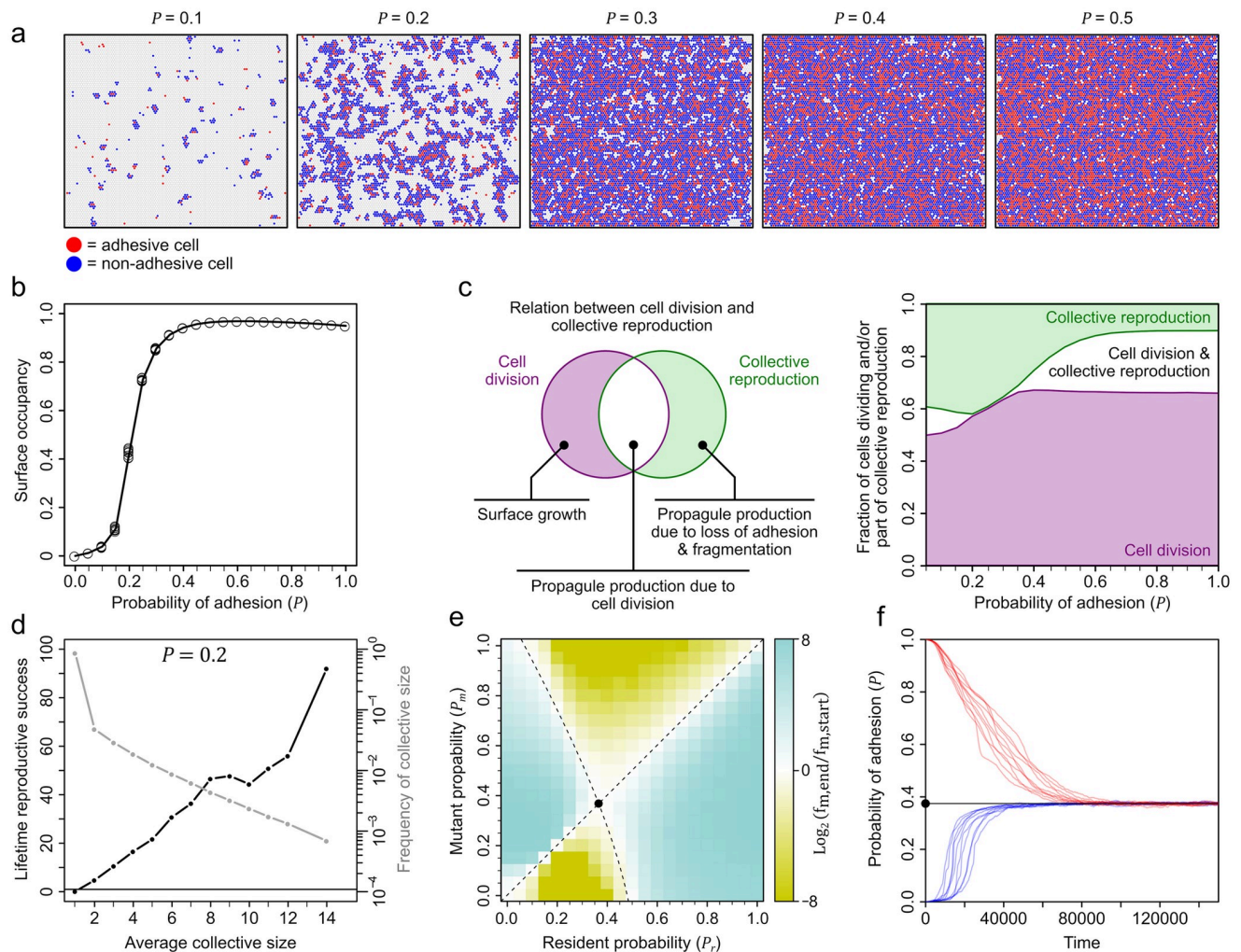


Fig 2. Relation between adhesion probability and collective properties. (a) Surface with adhesive (red) and nonadhesive (blue) cells at different adhesion probabilities. (b) Relation between surface occupancy and adhesion probability ($n = 10$). (c) Left, Venn diagram showing the conceptual relationship between cell division and collective reproduction: purple, cell division without collective reproduction, which results in collective growth; white, cell division that leads to detaching propagule; green, collective reproduction without cell division (e.g., fragmentation or propagule production due to loss of adhesion). (c) Right, fraction of cells on the surface that undergo cell division and/or are part of collective reproduction. (d) Relation between lifetime reproductive success and collective size (i.e., number of cells) for $P = 0.2$. (e) Pairwise invasibility analysis ($n = 10$, for every competition of resident and mutant genotypes): white, fitness of resident and mutant genotypes are the same; cyan, fitness of mutant genotype is higher; ocre, fitness of resident genotype higher (see S1 Text). Black dot, adhesion probability (P^*) favored in competition. Dashed lines show isoclines where resident and mutant genotypes are equally fit. (f) Evolution of adhesion probability in populations starting from $P = 0$ (blue lines; $n = 10$) and $P = 1$ (red lines; $n = 10$). Black vertical line: P^* . Raw data are provided in S2 Data in Github repository <https://github.com/jordivangestel/PLoS-Biology-2021>.

<https://doi.org/10.1371/journal.pbio.3001250.g002>

each collective on average produces a single offspring. We start by tracking all cell collectives at an adhesion probability of $P = 0.2$ (Fig 2d). This reveals that lifetime reproductive success strongly depends on collective size. Most collectives are small, consisting of a single cell only (86%), and have an average lifetime reproductive success of 0.13 offspring. In contrast, the largest collectives (consisting of 14 cells on average) are rare (0.06%) but have an enormous lifetime reproductive success of 92 offspring. This strong reproductive skew entails that large collectives contribute a disproportional number of offspring to future generations. Most of this offspring consists of single-cell propagules that are short lived and fail to reproduce.

Higher adhesion probabilities increase the fraction of large collectives, but simultaneously lower their reproductive output, due to the costs of adhesion (S3 Fig).

Thus, our model predicts that merely by varying the propensity to adhere, cells can give rise to diverse collectives that differ in size (Fig 2d, S2 and S3 Figs), mode of reproduction (Fig 2c), and lifetime reproductive success (Fig 2d and S3 Fig). These properties spontaneously arise through the interaction of cells on the surface and do not require any form of regulation, such as the expression of adhesion in response to collective size, as seen in many colony-forming bacteria [53]. Moreover, because collectives congregate on the surface, their properties are largely cryptic and cannot be distinguished by visually inspecting the surface at any moment in time. Only through lineage tracking can we identify individual collectives and study their properties [48].

Evolution of adhesion

So far, we studied how the adhesion probability affects the emergence of cell collectives on the surface. Next, we turn to the question how the adhesion probability itself might evolve. Given the strong reproductive skew in favor of large collectives, we predict that selection would favor higher adhesion probabilities, which lead to larger collectives, until the costs of adhesion no longer outweigh the benefits of growth. To find out, we allowed adhesion to vary by mutation in individual cells, as, for example, observed in many bacterial species [43,54–56]. We subsequently performed pairwise competitions between multiple combinations of mutant and resident genotypes, where a mutant has an adhesion probability of P_m and the resident of P_r . At the onset of competition, we assume that 10% of cells carry the mutant genotype and all cells occur in the bulk. We then determined whether the mutant increases in frequency during surface competition with the resident genotype. Fig 2e shows the results of all pairwise competitions, which reveals that selection favors an adhesion probability of $P^* \approx 0.4$. Lower adhesion probabilities ($P < P^*$) are selected against, because they result in smaller collectives (when $P_r < P^*$, $P_m > P_r$ can invade; Fig 2e and S3 Fig) and larger adhesion probabilities ($P > P^*$) are selected against, because they increase the cost of adhesion without increasing the collective size, due to a lack of space (when $P_r > P^*$, $P_m < P_r$ can invade; Fig 2e and S3 Fig).

To confirm that P^* is indeed favored by selection, we also performed evolutionary simulations. In these simulations, we start with a population of only adhesive cells ($P = 1$) or no adhesive cells ($P = 0$) and assume that dividing cells have a small probability of incurring a mutation that slightly alters the adhesion probability (S1 Text). We find that populations always converge to the same adhesion probability of $P^* = 0.37 \pm 0.004$ (mean \pm SD; $n = 100$) regardless of the initial conditions, which supports our pairwise competition analysis (Fig 2f). The exact adhesion probability that evolves, P^* , does depend on the variables such as the cost of adhesion. When adhesion cost increases, P^* decreases (S4 Fig).

In sum, our model predicts that surface colonization can rapidly evolve through mutations that affect the propensity to adhere. This prediction is corroborated by numerous laboratory experiments. For example, within days, *Pseudomonas fluorescence* cells can colonize the air-liquid interface, due to mutations that lead to the overproduction of an adhesive cellulosic polymer [54,57]. Similarly, within tens of generations, *B. subtilis* colonies can accumulate mutations that alter the fraction of adhesive cells in the population [58]. The ease by which adhesion evolves also has clinical implications [59]. For instance, during chronic lung infection of cystic fibrosis patients, *Pseudomonas aeruginosa* rapidly evolves mucoid colonies [55,60]. These colonies overproduce the adhesive polysaccharide alginate, which enhances surfaces attachment and increases antibiotic resistance [61]. Taken together, these studies emphasize the strong selective benefit of surface growth.

Evolution of regulation

Until now, we ignored the role of regulation in the evolution of surface colonization. Regulation, however, plays a critical role in the evolution of multicellularity, because it enables cells to coordinate their properties to the benefit of collective growth or reproduction [20,62–65]. Accordingly, in many surface-associated organisms, cells regulate the spatiotemporal expression of adhesion [18,66,67]. Cells can, for instance, tune the expression of adhesion depending on the adhesive molecules they sense in the collective, using so-called adhesion receptors [68]. Cells can also directly sense other cells within the collective, using so-called kin recognition systems, and adjust their adhesive properties in response [69,70]. Even primitive surface colonizers can have elaborate signal transduction cascades to control the expression of adhesion [71]. For example, in the bacterium *B. subtilis*, colony formation depends on communicative signals [72,73], osmotic stress [74], adhesive molecules [68], and nutrient stress [71]. Regulation affects when and where in a colony cells express adhesion and thereby also affects colony growth [21,22].

In this section, we examine how regulation impacts the evolution of surface colonization. For our purpose, we compare 3 idealized types of regulation, which we detail below (Fig 3a). In each type, we start with a population of nonadhesive cells and subsequently explore how the fraction of adhesive cells evolves in time. In addition, we examine how collectives are organized at the end of evolution, by quantifying (i) their size; (ii) their fraction of adhesive cells; and (iii) the spatial arrangement of those cells.

When adhesion is expressed stochastically and is not subject to regulation (type 1), we observe a rapid increase in the fraction of adhesive cells over evolutionary time, until the surface becomes fully occupied. The fraction of adhesive cells stabilizes to approximately one-third of the population (0.35 ± 0.006 ; mean \pm SD, $n = 100$; Fig 3b and 3c, S11 Movie). Collectives are strongly skewed in size, such that most consist of few cells (Fig 3d), and they show no signs of spatial organization (Fig 3e). That is, adhesive cells are not preferentially localized towards either the center or the periphery of collectives.

In modeling regulation, we follow experimental evidence by assuming that cells can detect adhesive molecules and regulate their own adhesion in response [68] (type 2). In many surface-associated organisms, cells use membrane-bound receptors to sense adhesive molecules [75–77]. These receptors can either bind to the adhesive molecules directly [68] or sense them indirectly through, for example, changes in the osmolarity [74]. To emulate these regulatory mechanisms, we assume that cells can increase or decrease the adhesion probability (P) in response to the fraction of adhesive neighbors (see Methods). We also assume that cells do not express adhesion at the onset of evolution. During evolution, they can accrue mutations that affect the adhesion probability (P) and its dependency on the fraction of adhesive neighbors by either increasing or decreasing P .

We first examine how regulation affects the fraction of adhesive cells and its change in evolutionary time. As in the absence of regulation, the fraction of adhesive cells initially increases, but then after a surface becomes fully occupied, the fraction steadily declines to a much lower value of approximately 0.19 ± 0.002 ($n = 100$) at the end of evolution. The decline in adhesive cells can be explained by the gradual evolution of a regulatory switch (Fig 3b), where cells become adhesive ($P \approx 1$) in the absence of adhesive neighbors and become nonadhesive ($P \approx 0$) otherwise. This switch assures that cells remain attached to the surface, while avoiding the costs of adhesion, because they only become adhesive when strictly necessary (i.e., in the absence of adhesive neighbors). When there are no costs associated with the expression of adhesion, the regulatory switch does not evolve (S4 Fig). The regulatory switch also affects the

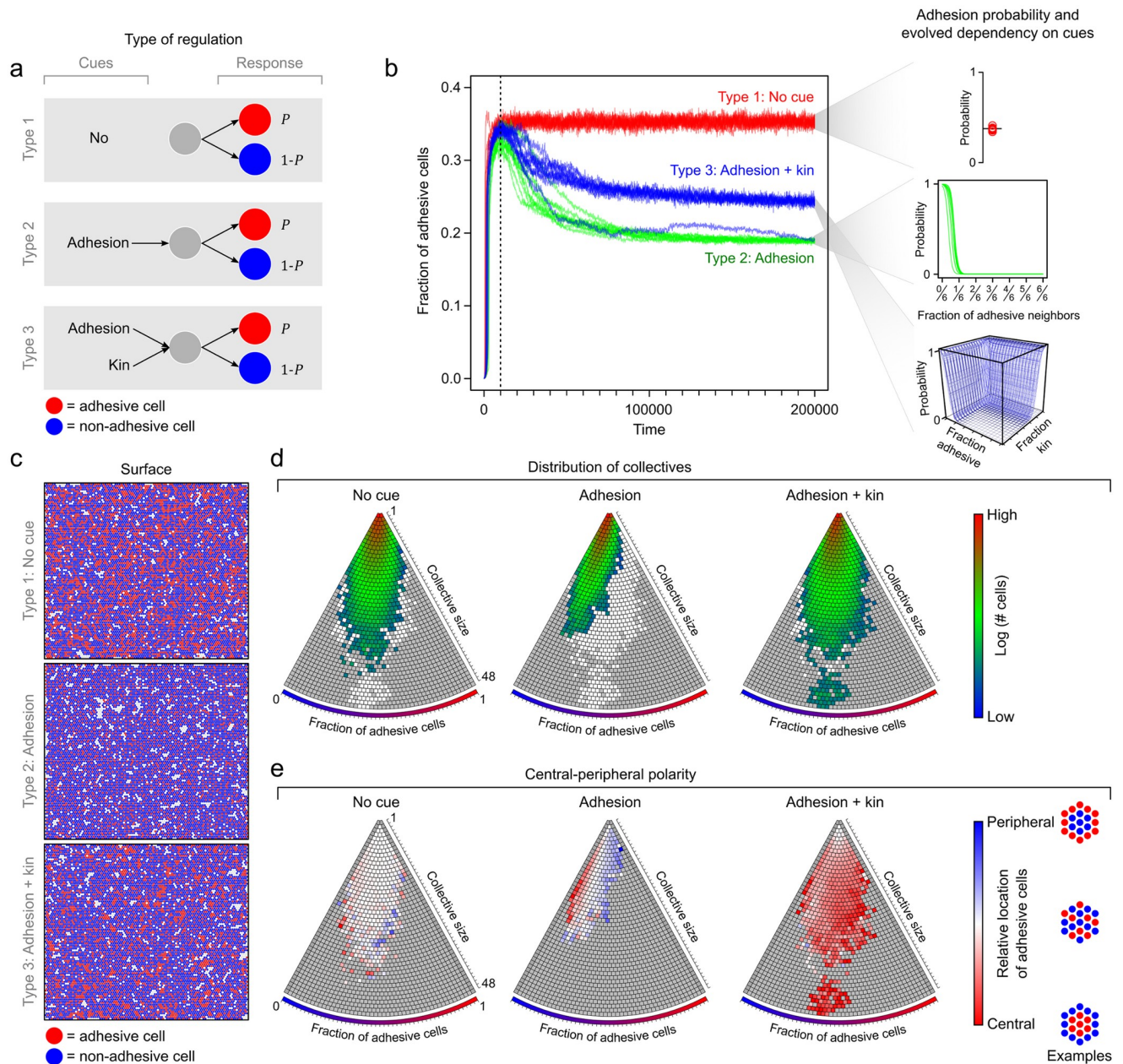


Fig 3. Type of regulation profoundly impacts evolution of cell collectives. (a) Schematic depiction of 3 idealized types of regulation. Cues that cells sense and the probability that cells become adhesive (P , red) or nonadhesive ($1 - P$, blue). (b) Left, fraction of adhesive cells in population over evolutionary time ($n = 10$; see also S6 Fig): red, type 1; green, type 2; blue, type 3. (b) Right, evolved dependency of adhesion probability on environmental cues ($n = 10$). (c) Surface at the end of evolution. (d) Distribution of collectives according to their size and the fraction of adhesive cells within the collective: grey, collectives that are never observed; white, collectives that are observed in other regulatory systems; color, log-transformed number of cells that are associated with observed collectives. (e) Central-peripheral polarity in cell adhesion: red, adhesive cells are localized closer to center than nonadhesive cells; blue, nonadhesive cells are localized closer to center than nonadhesive cells; white, no difference between localization of adhesive and nonadhesive cells. Note, since localization of adhesive cells is determined relative to that of nonadhesive cells, polarity can only be established for collective with both adhesive and nonadhesive cells.

<https://doi.org/10.1371/journal.pbio.3001250.g003>

spatial arrangement of cells within a collective (Fig 3e): If the fraction of adhesive cells is higher than average, they are localized towards the periphery of the collective, and when the fraction of adhesive cells is lower than average, they are localized towards the center. This spatial arrangement is concordant with a checkerboard pattern, where adhesive cells are equally

spaced out over the surface (Fig 3c, S7 Fig, and S12 Movie), as, for example, observed during epithelia development [78]. Thus, the regulation of adhesion strongly impacts both the fraction of adhesive cells inside a collective as well as their spatial arrangement. In contrast, in the absence of regulation, no such spatial organization can evolve, because cells have no information about their neighboring cells.

In addition to sensing adhesive molecules, we also examine the impact of kin recognition (type 3). Surface-associated organisms express a plethora of kin recognition mechanisms, from strain-specific communication systems to interlocking membrane-bound receptors [24,69,70,79–83]. These systems enable cells to sense kin, which—in the case of clonal growth—consist of closely related or genetically identical cells. Kin recognition systems can profoundly impact the organization of collectives, by facilitating cooperative interactions between cells [84]. For example, in many bacterial colonies, cells communicate by secreting diffusible quorum-sensing molecules whose concentration varies with colony size, which allows cells to respond to the colony size by for example inducing dispersal [53,85,86].

We here consider an idealized kin recognition system, where cells can sense the fraction of neighboring cells with the same genotype, thereby emulating a membrane-bound recognition system [69,87]. We define a cell's genotype by its regulatory response to its surrounding cells, such that cells from the same kin group have the same adhesion probability in any given environment. We do not address how kin recognition itself evolves, which has intensively been studied elsewhere [88–91], but instead explore how the presence of kin recognition, as observed in many surface-associated organisms, could potentially affect the evolution of collectivity. We implement kin recognition in addition to adhesion regulation, meaning that cells can sense both the fraction of adhesive cells and of kin in their neighborhood and either increase or decrease the adhesion probability in response (Methods).

Fig 3b shows how the fraction of adhesive cells changes over evolutionary time in this scenario. The fraction of adhesive cells first steeply increases and then slowly declines until, at the end of evolution, 0.25 ± 0.058 ($n = 100$) of the cells are adhesive, which is intermediate to the fraction of adhesive cells observed without regulation and with adhesion regulation alone ($\chi^2_{(2)} = 257.11$, $p < 10^{-16}$). In contrast to the other regulatory systems, the fraction of adhesive cells varies with the collective size: Small collectives have fewer adhesive cells than large collectives (S5 Fig; see also S13 Movie). This size-dependent adhesion can be explained by the evolved regulatory response (Fig 3b): Cells become adhesive ($P \approx 1$) when they have no adhesive neighbors or when they are surrounded by kin. Since cells in large collectives are more likely to be surrounded by kin than those in small collective, the fraction of adhesive cells increases with collective size, which mimics quorum-sensing responses seen in several bacterial species [53]. Intriguingly, kin recognition also leads to spatial polarity. Cells in the center of collectives are more likely to be surrounded by kin than those at the edge, which results in a central-peripheral polarity, in which adhesive cells are localized towards the center (Fig 3e).

The central-peripheral polarity strongly benefits collective growth: Adhesive cells in the center of the collective support the surrounding nonadhesive cells in staying attached to the surface. By avoiding the costs of adhesion, these nonadhesive cells have a competitive advantage in surface competition with neighboring collectives. Being surrounded by kin, the adhesive cells in the center are largely shielded from such competition (S7 Fig). Thus, even though the central-peripheral polarity increases the overall fraction of adhesive cells within a collective, and thereby the costs, it benefits surface growth by fostering a division of labor between adhesive and nonadhesive cells. The profound impact of this spatial organization on surface growth is perhaps best illustrated in a small fraction of the simulations (approximately 3%), where growth is so effective that one genotype monopolizes nearly the entire surface, causing a

massive collapse in genetic diversity and a steep increase in the overall fraction of adhesive cells (S6 Fig).

Besides analyzing the properties of collectives at the end of evolution, we also examined their growth dynamics in time (S3 Text). Irrespective of the type of regulation, we observe that collectives undergo diverse conformational changes in time, affecting both their size and form (S3 Text, S8–S12 Figs). In contrast to these diverse growth dynamics, reproduction mostly occurs through single-cell propagules (S13 Fig). These results broadly mimic the growth patterns of primitive surface colonizers in nature, where growth opportunities on the surface determine the exact size and form of collectives, but where collectives nevertheless express a consistent spatial organization, like the central-peripheral polarity observed in this study [33,36,92,93].

In summary, our model predicts that regulation of adhesion can strongly impact collective growth. Specifically, we observe that the evolution of a central-peripheral polarity in cell adhesion fosters the division of labor between adhesive and nonadhesive cells. In *B. subtilis*, a very similar division of labor has been observed [21,94]: Cells in the colony center produce a costly molecule, surfactin, that promotes surface growth of cells at the periphery. Like in our model, where the central-peripheral polarity depends on kin recognition, surfactin production is triggered by a kin-specific quorum-sensing signal [26,95,96]. We postulate that central-peripheral polarity may form a generic organizing principle that profits surface growth, because it allows cells at the border to specialize in surface competition, while being supported by cells in the center. For that reason, it might not be surprising that kin recognition systems are widely observed in surface-associated organisms, from primitive colony-forming bacteria like *B. subtilis* to colonial animals [24,69,70,79–81].

Discussion

In this study, we showed how a primitive form of surface-associated multicellularity can readily evolve in the presence of two commonly observed cell-level properties: cell adhesion and the regulatory control of adhesion. By merely evolving the propensity to adhere, cells rapidly colonize a surface, where they form primitive cell collectives (step 1 in Fig 4). These first collectives show no consistent spatial organization and closely resemble forms of bacterial surface colonization that can spontaneously evolve in the lab [43,54,60]. Collectives nevertheless express diverse properties, differing in size, mode of propagation, and lifetime reproductive success. A strong reproductive skew in favor of large collectives drives the evolution of adhesion. Then, through kin recognition, collectives evolve a central-peripheral polarity in cell adhesion (step 2 in Fig 4). This simple multicellular organization profoundly impacts surface growth by facilitating a division of labor between adhesive and nonadhesive cells (S6 Fig).

Throughout their evolution, collectives retain a largely cryptic appearance (see Fig 3c). That is, when visually inspecting a surface, one would not be able to distinguish between neighboring collectives, because there are no morphological boundaries that separate them. Lineage tracking is the only means to identify and examine such primitive surface-associated collectives. Our modeling approach contrasts with previous models on the evolution of multicellularity, which did not apply lineage tracking. For instance, many evolutionary models start by assuming the presence of physically separated collectives. These models do not address how collectives emerge, but instead ask how—after their origination—collectives evolve properties important for multicellular organization, such as cooperation [9,97,98] or division of labor [99–101]. Similarly, many developmental models consider collectives in isolation and ask how cells can give rise to collective properties through self-organization [40,102–104]. Finally, there is a large group of models that, like ours, study how cells interact and evolve on a surface

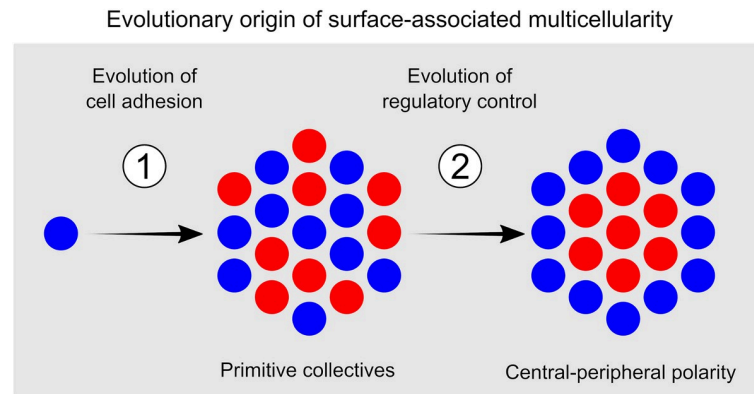


Fig 4. Proposed evolutionary origin of surface-associated multicellularity. First, cell adhesion evolves, leading to cryptic cell collectives on a surface. Second, regulation evolves which leads to central-peripheral polarity, which brings about a characteristic collective organization.

<https://doi.org/10.1371/journal.pbio.3001250.g004>

[105–109]. As cells divide and die on a surface, they spontaneously give rise to collectives, but instead of tracking these collectives, most models revert their attention to the underlying genotypes and ask what genotypes prevail over evolutionary time [105–109]. As a result, it often remains unclear how the earliest surface-associated cell collectives are organized and how this organization subsequently affects a collective’s competitive success in terms of surface growth and reproduction. In contrast, our model makes some concrete predictions about emergent cell collectives. For instance, it predicts that, at least initially, collectives are strongly skewed in size, with a few large collectives producing most single-cell propagules. In addition, our model predicts that a central-peripheral polarity in cell adhesion can result in a strong competitive advantage, sometimes leading to a few genotypes monopolizing the entire surface. An exciting task for future work is to validate these predictions experimentally.

Theoretical models on surface growth are paralleled by a large body of empirical literature where surface-associated organisms are studied by either growing collectives in isolation (e.g., biofilms, colonies, pellicles, swarms, fruiting bodies) [110–113], thereby focusing on their multicellular organization [36,114–118], or by competing several genotypes against each other on a surface [30,119–124]. Competition experiments revealed that spatial interactions can strongly affect the outcome of competition, oftentimes leading to the coexistence of multiple genotypes [43,120,125]. However, due to technical challenges and the transient nature of many primitive cell collectives [126], there is often a limited quantitative understanding of how genotypes exactly give rise to individual cell collectives and how these collectives subsequently grow and propagate in competition with other collectives. Since the spatiotemporal organization of collectives determines a genotype’s competitive success (i.e., rates of collective growth and reproduction)—making collectives the relevant unit of biological organization [49,50]—we need to understand how collective organization comes about to uncover how primitive forms of surface-associated multicellularity first arise and subsequent evolve.

Fortunately, over the last decade, methods of empirical lineage tracking have strongly improved through advances in single-cell microscopy [126–128], image analysis [129], single-cell sequencing [51,130,131], and genome editing [132,133], thereby opening up the possibility of studying primitive cell collectives across a wide range of organisms [126]. For example, the stochastic and combinatorial expression of fluorescent proteins makes it possible to trace up to approximately 100 lineages without interrupting the spatial configuration of cells [134]. Moreover, recent developments combining barcoding with fluorescence in situ hybridization have

increased the spatial resolution at which cell lineage can be traced [135] and dual-view light sheet microscopy has made it possible to track entire cell populations in real time without interruption [127,136]. Finally, advances in spatial transcriptomics make it possible to simultaneously examine the expression of hundreds of genes in space, which, for instance, revealed that bacteria cells can express vastly distinct expression profiles within the same colony [137]. Currently, most of the above technologies are applied to study a few genetically tractable model organisms, but they hold the promise of uncovering many still hidden forms of multicellular organization in nonmodel organisms as well.

Cryptic origins of biological organization exist on all spatiotemporal scales. On the smallest scale, the spatial organization of an embryo is often laid out through an asymmetric distribution of patterning molecules in a developing oocyte, long before embryonic development creates any visible spatial organization [138,139]. On the largest scale, reproductive isolation often exists in cryptic species with little or no apparent morphological or ecological differences [140,141]. Suitable experimental technologies are essential to reveal such hidden differences and understand the evolutionary origins of crypticity [140]. To identify cryptic multicellularity, these technologies involve state-of-the-art lineage tracking methods, which can uncover a hidden diversity of surface-associated multicellularity, both primitive and advanced. Given how few and widely met prerequisites our model needs to create multicellular organization, we expect that cryptic multicellularity will be widespread and that it will originate long before the first multicellular individuals become morphologically evident.

Methods

We study the early emergence of surface-associated multicellularity using an individual-based model, which builds on a previous model of surface colonization [41]. The model emulates an ecology where cells can occupy 2 possible environments: the bulk and the surface. The bulk is a three-dimensional space above the surface (e.g., water column), where cells can freely move around but cannot adhere to each other. Cells can attach to the surface through adhesion. The surface is represented by a hexagonal grid of 100×100 grid elements (see [S1 Text](#) of an detailed discussion on alternative surface geometries). Each grid element can be occupied by a single cell, which can have up to 6 neighboring cells. In total, the surface can therefore be colonized by 10,000 cells.

In the model, we only account for cell-level events and use spatial lineage tracking (see [S2 Text](#)) to determine how collectives spontaneously emerge on the surface. Cells can express 2 distinct phenotypes, adhesive or nonadhesive, and can undergo 1 of 5 possible events at every timestep: (1) surface attachment; (2) surface detachment; (3) cell division; (4) cell death; and (5) phenotypic change in adhesion. [S1 Text](#) details each of these events. In short, cells can attach to a surface when they are adhesive or associate with an adhesive cell on the surface. We thereby assume that adhesion mediates both cell–surface and cell–cell contact. Cells detach when they are nonadhesive and not associated with an adhesive neighbor. Cell division depends on both the environment in which cells occur (surface versus bulk) and their phenotype (adhesive versus nonadhesive). In the bulk, cells can only divide when the population size is below a predetermined carrying capacity ($K_{bulk} = 5,000$ cells). On the surface, cells can divide whenever there is space in one of the neighboring grid elements. After division on the surface, a cell could remain attached or it could immediately detach to the bulk. Because adhesion is known to be costly, we assume that adhesive cells have lower cell division rate than nonadhesive cells, irrespective of the environment. In our evolutionary simulations, cells have a small probability of incurring a mutation at every cell division (for details, see [S1 Text](#)). Cell death occurs with a fixed probability, irrespective of the environment and phenotype of cells. Finally,

cells can change their phenotype: With a probability P , a cell becomes or remains adhesive, and with a probability $1 - P$, a cell becomes or remains nonadhesive. Depending on the simulations, the adhesion probability (P) is either unchanging (Fig 2a–2e) or subject to evolutionary change (Figs 2f and 3). In addition, depending on the type of regulation (Fig 3), the adhesion probability can depend on the fraction of adhesive cells and fraction of kin (see S1 Text for details on the adhesion probability).

At the onset of the simulations, we assume that cells occur in the bulk and that none of them is adhesive. Unless specified otherwise, we perform nonevolutionary simulations (Fig 2), where cells have a fixed adhesion probability, for 1,000 timesteps (T_{max}), which equals approximately 20 cell generations. We perform evolutionary simulations (Figs 2f and 3) for 200,000 timesteps, which equals approximately 4,000 cell generations. For further parameter values, see S1 Text. Since the model only accounts for cell-level events, we monitor collectives by following their constituent cells in time. In this way, we can determine how collectives first appear on a surface through cell attachment and subsequently grow and reproduce. We measure various collective properties, including collective size, spatial organization, and life span. In S2 Text, we specify how each cell-level event can affect the processes of collective growth and reproduction. In short, collective growth results from cell division on the surface, where a daughter cell remains surface-attached next to the mother cell. Collective reproduction can result from cell division, surface detachment, or cell death. Cell division and surface detachment result in propagule production, where a (daughter) cell that detaches to the bulk forms a propagule of the collective on the surface. Surface detachment and cell death can lead to fragmentation, where a collective of formerly connected cells splits up in 2 or more smaller collectives.

Supporting information

S1 Fig. Relation between cell-level events and collective reproduction and growth. (a) Scenario 1: cell death leading to collective reproduction through fragmentation. Cell death (yellow) can lead to the fragmentation of 2 groups of previously connected cells. (b) Scenario 2: cell detachment leading to reproduction. The detaching cell forms a propagule that originates from within a collective. Detachment can also lead to fragmentation of 2 groups of previously connected cells. (c) Scenario 3: cell division leading to collective reproduction. On a surface, cell division can lead to propagule production when a daughter cell does not remain attached. In the bulk, cells are never associated, so cell division by definition results in reproduction. Note that in the bulk, cells are counted as single cell “collectives.” (d) Scenario 4: cell division leading to collective growth when a daughter cell remains attached to the surface.

(TIF)

S2 Fig. Surface colonization and cell collectives. (a) Surface at end of simulations with adhesive (red) and nonadhesive (blue) cells at $P = [0.1, 1]$. (b) Representative cell collectives traced from birth till death (see also Fig 1d): lines, cell lineage underlying cell collective showing both adhesive (red) and nonadhesive (blue) cells; branches, cell division; light green dots, collective offspring resulting from fragmentation; dark green dots, collective offspring resulting from propagule production; green convex hull illustrates relative size of collective. Offspring are not traced in time. Cell lineages show relative location of cells within the collective.

(TIF)

S3 Fig. Lifetime reproductive success increases with collective size. Lifetime reproductive success (left y axis) is determined by the total number of offspring resulting from either propagule production or fragmentation (Fig 1c), produced over the life span of a collective. Average

collective size (x axis) refers to the average number of cells that constitute a collective over the life span of the collective. Frequency of collectives (right y axis) with given size. Blue, purple, and red, probability (P) that cells express adhesion of respectively 0.2, 0.4, and 0.6. Raw data are provided in [S2 Data](#) in Github repository <https://github.com/jordivangestel/PLoS-Biology-2021>.

(TIF)

S4 Fig. Reaction norms that evolved at different adhesion costs. Reaction norms ($n = 5$) of most abundant genotypes at the end of evolution for different costs of adhesion, where the cost of adhesion is defined by the cell division rate of adhesive cells relative to that of nonadhesive cells. Each reaction norm shows the probability of adhesion (P) as a function of both the fraction of adhesive cells and the fraction of kin in a cell's neighborhood (i.e., the 6 neighboring positions surrounding a cell on the hexagonal surface). Irrespective of the type of regulation, when the costs of adhesion increase (i.e., lower cell division rate of adhesive cells), the probability of adhesion decreases (i.e., reaction norms color less red and more blue). Within each type of regulation, the shape of the reaction norm remains qualitatively the same for a wide range of adhesion costs. Top-bottom, reaction norms associated with type 1, 2, and 3 regulation.

(TIF)

S5 Fig. Relation between fraction of adhesive cell and collective size. Average fraction of adhesive cells in collectives of different size for type 1 (red), 2 (green), and 3 (blue) regulation. Only in type 3 regulation there is a strong increase in the fraction of adhesive cells when collectives increase in size, while there is only a weak increase for the other types of regulation. Raw data are provided in [S2 Data](#) in Github repository <https://github.com/jordivangestel/PLoS-Biology-2021>.

(TIF)

S6 Fig. Evolution of type 3 regulation leads to 3 alternative evolutionary outcomes. (a) Average fraction of adhesive cells in 100 independent simulations of different type of regulation: red, no cue; green, adhesion only regulation; red, adhesion regulation + kin recognition. (b and c) Detailed analysis of simulations in type 3 regulation. In type 3 simulations, we observe 3 alternative evolutionary outcomes, where fraction of adhesive cells on the surface is (outcome 1, light blue) low, (outcome 2, blue) intermediate, or (outcome 3, dark blue) high. In outcome 1 (3/100 simulations; light blue), kin recognition does not evolve; cells therefore behave the same as those in adhesion only regulation (type 2), which results in a low fraction of adhesive cells on the surface (b). In outcome 2 (94/100, blue), kin recognition evolves, and cells behave as described in the main text ([Fig 3](#)), resulting in an intermediate fraction of adhesive cells (b). In outcome 3 (3/100), kin recognition evolves and leads to the dominance of one genotype on the surface. This results in a high fraction of adhesive cells because most cells are surrounded by kin (b). Since one genotype monopolizes the surface, it also results in a collapse of the genotypic diversity in the population, as shown by a strong reduction in the Shannon diversity shown in panel c.

(TIF)

S7 Fig. Clusters of interconnective adhesive cells on the surface are most similar in type 3 regulation. (a) Examination of the diversity underlying clusters of interconnected adhesive cells (directly neighboring each other) on the surface at the end of evolution. For each cluster, we analyze cells one by one and determine their genotype and the collectives to which they belong. Based on this, we calculate the underlying Shannon diversity ($H = -\sum p_i \cdot \ln p_i$). When all cells in the cluster have the same genotype, the Shannon diversity of genotypes is 0. By the same token, when all cells in the cluster belong to the same collective, the Shannon diversity of

collectives is 0. When the Shannon diversity of collectives is higher than 0, it means that the clusters of interconnected cells consists of multiple collectives that merged on the surface. Box-plots in (a) show median Shannon diversity (horizontal black line), interquartile range (box), data within 1.5 times interquartile range above the upper quartile and below the lower quartile (whiskers) and outliers. The diversity analysis uncovers two main findings: First, clusters of interconnected adhesive cells are most homogeneous in type 3 regulation, meaning that they more often consist of cells with the same genotype and cells belonging to the same collective. Thus, in the presence of kin recognition, adhesive cells are more likely to be surrounded by kin than in the absence of kin recognition. Second, for all types of regulation and clusters sizes, the diversity of genotypes is lower than the diversity of collectives, meaning that clusters often consist of multiple collectives that merged on the surface but have the same genotype (hence increasing the diversity of collectives underlying a cluster but not the diversity of genotypes). (b) Surface at the end of evolution for different types of regulation, revealing clusters of interconnected adhesive cells on the surface (i.e., clusters of red cells). Raw data are provided in [S2 Data](#) in Github repository <https://github.com/jordivangestel/PLoS-Biology-2021>. (TIF)

S8 Fig. Procedure for identifying spatial configurations. First, all collectives are extracted from the surface, as indicated by the different numbers. Second, the spatial configuration of each collective is determined by examining the spatial location of both adhesive (red) and non-adhesive cells (blue) within the collective. Third, the spatial configurations are compared between collectives to identify all unique configurations, thereby correcting for radial symmetry. This results in a list of unique spatial configurations together with the number of collectives that display each spatial configuration. (TIF)

S9 Fig. Spatial configuration of collectives can be characterized by their size and fraction of adhesive cells. (a) Each node corresponds to a unique spatial configuration that is expressed by at least 100 of $5 \cdot 10^7$ analyzed collectives. The distance between two nodes is determined by their similarity (see [Methods](#)). The node size corresponds to the number of collectives that express the associated spatial configuration. (b) Collective size of different spatial configurations. (c) Fraction of adhesive cells in spatial configuration. (TIF)

S10 Fig. Collectives from different types of regulation express different spatial configurations. For each spatial configuration (i.e., node in the network), we determine how frequently it is observed among collectives from each type of regulation. This reveals that small collectives with many adhesive cells are more commonly observed in type 1 regulation (a, red), collectives with low fraction of adhesive cells are more commonly observed in type 2 regulation (b, green) and large collectives are more commonly observed in type 3 regulation (c, blue). (TIF)

S11 Fig. Type of regulation affects how collectives change their spatial configuration in time. Transparent nodes show unique spatial configurations, like shown in [S9](#) and [S10](#) Figs. Connections show how collectives change their spatial configuration in time (see also [S12 Fig](#) for individual examples). Color shows frequency by which change in spatial configuration is observed in different types of regulation: red, changes mostly observed in type 1 regulation; green, changes mostly observed in type 2 regulation; blue, changes mostly observed in type 3 regulation. (TIF)

S12 Fig. Examples of how collectives change their spatial configuration in time from their origin till the moment they first reproduce. Each panel shows an example of how a collective in one of the 3 regulatory systems changes its spatial configuration in time. In each example, the collective is seeded by a nonadhesive cell, which grows on the surface and thereby gives rise to different spatial configurations. Upper, bold black lines show within the network representation how a collective changes its spatial configuration in time. Below, small representations of collective show how the spatial configuration of the collective changes in time. We trace each collective until the first successful reproductive event that leads to a nonadhesive propagule (small grey arrow), thereby completing the life cycle. (a) Example of how collective changes its spatial configuration in the type 1 regulation. (b) Example of how collective changes its spatial configuration in the type 2 regulation. (c) Example of how collective changes its spatial configuration in the type 3 regulation.

(TIF)

S13 Fig. Most offspring collectives are nonadhesive single-cell propagules. (a) Lines connect spatial configuration of parental collectives and offspring collectives upon reproduction. (b) Red nodes highlight spatial configuration of offspring collectives. The frequency by which a configuration is observed is indicated by the saturation of the fill color. Most offspring collectives have the same spatial configuration: nonadhesive single-cell propagules (see also [S9 Fig](#)).

(TIF)

S1 Movie. Surface colonization with 10% probability of expressing adhesion.

(MP4)

S2 Movie. Surface colonization with 20% probability of expressing adhesion.

(MP4)

S3 Movie. Surface colonization with 30% probability of expressing adhesion.

(MP4)

S4 Movie. Surface colonization with 40% probability of expressing adhesion.

(MP4)

S5 Movie. Surface colonization with 50% probability of expressing adhesion.

(MP4)

S6 Movie. Surface colonization with 60% probability of expressing adhesion.

(MP4)

S7 Movie. Surface colonization with 70% probability of expressing adhesion.

(MP4)

S8 Movie. Surface colonization with 80% probability of expressing adhesion.

(MP4)

S9 Movie. Surface colonization with 90% probability of expressing adhesion.

(MP4)

S10 Movie. Surface colonization with 100% probability of expressing adhesion.

(MP4)

S11 Movie. Surface colonization in evolved type 1 regulation.

(MP4)

S12 Movie. Surface colonization in evolved type 2 regulation.

(MP4)

S13 Movie. Surface colonization in evolved type 3 regulation.
(MP4)

S1 Text. Model. Description of model, which includes a description of all cell level events, determination of the adhesion probability for the 3 different types of regulation, pseudocode, simulation conditions, and a discussion on the role of the surface geometry.
(PDF)

S2 Text. Spatial lineage tracking. Description of collective growth, reproduction, and death.
(PDF)

S3 Text. Growth dynamics of collectives. Analysis of growth dynamics of collectives.
(PDF)

S1 Data. C++ code available from the Github repository <https://github.com/jordivangestel/PLoS-Biology-2021>.
(ZIP)

S2 Data. Raw data of summary figures available from the Github repository <https://github.com/jordivangestel/PLoS-Biology-2021>.
(XLSX)

Acknowledgments

We thank members of the Andreas Wagner Laboratory for fruitful discussions.

Author Contributions

Conceptualization: Jordi van Gestel, Andreas Wagner.

Formal analysis: Jordi van Gestel.

Funding acquisition: Jordi van Gestel, Andreas Wagner.

Investigation: Jordi van Gestel.

Methodology: Jordi van Gestel.

Project administration: Jordi van Gestel.

Resources: Jordi van Gestel, Andreas Wagner.

Supervision: Andreas Wagner.

Validation: Jordi van Gestel.

Visualization: Jordi van Gestel, Andreas Wagner.

Writing – original draft: Jordi van Gestel.

Writing – review & editing: Jordi van Gestel, Andreas Wagner.

References

1. Fusco G, Minelli A. The Biology of Reproduction. Cambridge, United Kingdom: Cambridge University Press; 2019.
2. Parsek MR, Fuqua C. Biofilms 2003: Emerging themes and challenges in studies of surface-associated microbial life. *J Bacteriol.* 2004; 186:4427–40. <https://doi.org/10.1128/JB.186.14.4427-4440.2004> PMID: 15231774
3. Buss LW. The Evolution of Individuality. Princeton: Princeton University Press; 1987.

4. Simpson C, Herrera-Cubilla A, Jackson JBC. How colonial animals evolve. *Sci Adv.* 2020; 6: eaaw9530. <https://doi.org/10.1126/sciadv.aaw9530> PMID: 31934622
5. Bonner JT. *First signals: the evolution of multicellular development.* Princeton: Princeton University Press; 2000.
6. Buss LW. Slime molds, ascidians, and the utility of evolutionary theory. *Proc Natl Acad Sci U S A.* 1999; 96:8801–3. <https://doi.org/10.1073/pnas.96.16.8801> PMID: 10430843
7. Buss LW. Evolution, development, and the units of selection. *Proc Natl Acad Sci U S A.* 1983; 80:1387–91. <https://doi.org/10.1073/pnas.80.5.1387> PMID: 6572396
8. Wilson DS. A theory of group selection. *Proc Natl Acad Sci U S A.* 1975; 72:143–6. <https://doi.org/10.1073/pnas.72.1.143> PMID: 1054490
9. Damuth J, Heisler IL. Alternative formulations of multilevel selection. *Biol Philos.* 1988; 3:407–30. <https://doi.org/10.1007/BF00647962>
10. Maynard Smith J. Group selection and kin selection. *Nature.* 1964; 201:1145–7. <https://doi.org/10.1038/2011145a0>
11. Bourke AFG. *Principles of Social Evolution.* Oxford, United Kingdom: Oxford University Press; 2011.
12. Hamilton WD. The evolution of altruistic behavior. *Am Nat.* 1963; 97:354–6. <https://doi.org/10.1086/497114>
13. Calcott B, Sterelny K. *The Major Transitions in Evolution Revisited.* Cambridge, Massachusetts: MIT Press; 2011.
14. Nadell CD, Drescher K, Wingreen NS, Bassler BL. Extracellular matrix structure governs invasion resistance in bacterial biofilms. *ISME J.* 2015; 9:1700–9. <https://doi.org/10.1038/ismej.2014.246> PMID: 25603396
15. Ramos Y, Rocha J, Hael AL, van Gestel J, Vlamakis H, Cywes-Bentley C, et al. PolyGlcNAc-containing exopolymers enable surface penetration by non-motile *Enterococcus faecalis*. *PLoS Pathog.* 2019; 15:e1007571. <https://doi.org/10.1371/journal.ppat.1007571> PMID: 30742693
16. Berk V, Fong JCN, Dempsey GT, Develioglu ON, Zhuang X, Liphardt J, et al. Molecular architecture and assembly principles of *Vibrio cholerae* biofilms. *Science.* 2012; 337:236–9. <https://doi.org/10.1126/science.1222981> PMID: 22798614
17. Hartmann R, Singh PK, Pearce P, Mok R, Song B, Díaz-Pascual F, et al. Emergence of three-dimensional order and structure in growing biofilms. *Nat Phys.* 2019; 15:251–6. <https://doi.org/10.1038/s41567-018-0356-9> PMID: 31156716
18. Abedin M, King N. Diverse evolutionary paths to cell adhesion. *Trends Cell Biol.* 2010; 20:734–42. <https://doi.org/10.1016/j.tcb.2010.08.002> PMID: 20817460
19. Heras B, Totsika M, Peters KM, Paxman JJ, Gee CL, Jarrott RJ, et al. The antigen 43 structure reveals a molecular Velcro-like mechanism of autotransporter-mediated bacterial clumping. *Proc Natl Acad Sci U S A.* 2014; 111:457–62. <https://doi.org/10.1073/pnas.1311592111> PMID: 24335802
20. Islam ST, Alvarez IV, Saïdi F, Guiseppi A, Vinogradov E, Sharma G, et al. Modulation of bacterial multicellularity via spatio-specific polysaccharide secretion. *PLoS Biol.* 2020; 18: e3000728. <https://doi.org/10.1371/journal.pbio.3000728> PMID: 32516311
21. van Gestel J, Vlamakis H, Kolter R. From cell differentiation to cell collectives: *Bacillus subtilis* uses division of labor to migrate. *PLoS Biol.* 2015; 13:e1002141. <https://doi.org/10.1371/journal.pbio.1002141> PMID: 25894589
22. Vlamakis H, Aguilar C, Losick R, Kolter R. Control of cell fate by the formation of an architecturally complex bacterial community. *Genes Dev.* 2008; 22:945–53. <https://doi.org/10.1101/gad.1645008> PMID: 18381896
23. Hawver LA, Jung SA, Ng WL. Specificity and complexity in bacterial quorum-sensing systems. *FEMS Microbiol Rev.* 2016; 40:738–52. <https://doi.org/10.1093/femsre/fuw014> PMID: 27354348
24. Wall D. Kin recognition in bacteria. *Annu Rev Microbiol.* 2016; 70:143–60. <https://doi.org/10.1146/annurev-micro-102215-095325> PMID: 27359217
25. Tran LSP, Nagai T, Itoh Y. Divergent structure of the ComQXPA quorum-sensing components: molecular basis of strain-specific communication mechanism in *Bacillus subtilis*. *Mol Microbiol.* 2000; 37:1159–71. <https://doi.org/10.1046/j.1365-2958.2000.02069.x> PMID: 10972833
26. Aframian N, Eldar A. A bacterial tower of babel: quorum-sensing signaling diversity and its evolution. *Annu Rev Microbiol.* 2020; 74:587–606. <https://doi.org/10.1146/annurev-micro-012220-063740> PMID: 32680450
27. Rutherford ST, Bassler BL. Bacterial quorum sensing: its role in virulence and possibilities for its control. *Cold Spring Harb Perspect Med.* 2012; 2. <https://doi.org/10.1101/cshperspect.a012427> PMID: 23125205

28. Libby E, Rainey PB. A conceptual framework for the evolutionary origins of multicellularity. *Phys Biol*. 2013; 10:035001. <https://doi.org/10.1088/1478-3975/10/3/035001> PMID: 23735467
29. Hammerschmidt K, Rose CJ, Kerr B, Rainey PB. Life cycles, fitness decoupling and the evolution of multicellularity. *Nature*. 2014; 515:75–9. <https://doi.org/10.1038/nature13884> PMID: 25373677
30. Nadell CD, Bassler BL. A fitness trade-off between local competition and dispersal in *Vibrio cholerae* biofilms. *Proc Natl Acad Sci U S A*. 2011; 108:14181–5. <https://doi.org/10.1073/pnas.1111147108> PMID: 21825170
31. Staps M, van Gestel J, Tarnita CE. Emergence of diverse life cycles and life histories at the origin of multicellularity. *Nat. Ecol Evol*. 2019; 3:1197–205. <https://doi.org/10.1038/s41559-019-0940-0> PMID: 31285576
32. Yan J, Nadell CD, Bassler BL. Environmental fluctuation governs selection for plasticity in biofilm production. *ISME J*. 2017; 11:1569–77. <https://doi.org/10.1038/ismej.2017.33> PMID: 28338673
33. Rumbaugh KP, Sauer K. Biofilm dispersion. *Nat Rev Microbiol*. 2020:1–16.
34. Boles BR, Horswill AR. *agr*-mediated dispersal of *Staphylococcus aureus* biofilms. *PLoS Pathog*. 2008; 4:e1000052. <https://doi.org/10.1371/journal.ppat.1000052> PMID: 18437240
35. Kragh KN, Hutchison JB, Melaugh G, Rodesney C, Roberts AEL, Irie Y, et al. Role of multicellular aggregates in biofilm formation. *MBio*. 2016; 7. <https://doi.org/10.1128/mBio.00237-16> PMID: 27006463
36. Claessen D, Rozen DE, Kuipers OP, S gaard-Andersen L, van Wezel GP. Bacterial solutions to multicellularity: a tale of biofilms, filaments and fruiting bodies. *Nat Rev Micro*. 2014; 12:115–24. <https://doi.org/10.1038/nrmicro3178> PMID: 24384602
37. Jelsbak L, S gaard-Andersen L. Pattern formation: fruiting body morphogenesis in *Myxococcus xanthus*. *Curr Opin Microbiol*. 2000; 3:637–42. [https://doi.org/10.1016/s1369-5274\(00\)00153-3](https://doi.org/10.1016/s1369-5274(00)00153-3) PMID: 11121786
38. Bonner JT. *The Social Amoebae: The Biology of Cellular Slime Molds*. Princeton, NJ: Princeton University Press; 2009.
39. van Gestel J, Tarnita CE. On the origin of biological construction, with a focus on multicellularity. *Proc Natl Acad Sci U S A*. 2017; 114:11018–26. <https://doi.org/10.1073/pnas.1704631114> PMID: 28973893
40. Hogeweg P. Evolving mechanisms of morphogenesis: on the interplay between differential adhesion and cell differentiation. *J Theor Biol*. 2000; 203:317–33. <https://doi.org/10.1006/jtbi.2000.1087> PMID: 10736211
41. van Gestel J, Nowak MA. Phenotypic heterogeneity and the evolution of bacterial life cycles. *PLoS Comput Biol*. 2016; 12:e1004764. <https://doi.org/10.1371/journal.pcbi.1004764> PMID: 26894881
42. Rainey PB, Rainey K. Evolution of cooperation and conflict in experimental bacterial populations. *Nature*. 2003; 425:72–4. <https://doi.org/10.1038/nature01906> PMID: 12955142
43. Drago  A, Martin M, Falc n Garc a C, Kricks L, Pausch P, Heimerl T, et al. Collapse of genetic division of labour and evolution of autonomy in pellicle biofilms. *Nat Microbiol*. 2018; 3:1451–60. <https://doi.org/10.1038/s41564-018-0263-y> PMID: 30297741
44. van Gestel J, Weissing FJ, Kuipers OP, Kov acs  T. Density of founder cells affects spatial pattern formation and cooperation in *Bacillus subtilis* biofilms. *ISME J*. 2014; 8:2069–79. <https://doi.org/10.1038/ismej.2014.52> PMID: 24694715
45. Velicer GJ, Yu YTN. Evolution of novel cooperative swarming in the bacterium *Myxococcus xanthus*. *Nature*. 2003; 425:75–8. <https://doi.org/10.1038/nature01908> PMID: 12955143
46. Norman TM, Lord ND, Paulsson J, Losick R. Stochastic switching of cell fate in microbes. *Annu Rev Microbiol*. 2015; 69:381–403. <https://doi.org/10.1146/annurev-micro-091213-112852> PMID: 26332088
47. Norman TM, Lord ND, Paulsson J, Losick R. Memory and modularity in cell-fate decision making. *Nature*. 2013; 503:481–6. <https://doi.org/10.1038/nature12804> PMID: 24256735
48. Griesemer J. Tracking organic processes: Representations and research styles in classical embryology and genetics. *From Embryology to Evo-Devo: A History of Developmental Evolution*. Cambridge, Massachusetts: MIT Press; 2007. pp. 375–433.
49. Griesemer J. The units of evolutionary transition. *Selection*. 2001; 1:67–80. <https://doi.org/10.1556/Select.1.2000.1-3.7>
50. Griesemer J. Development, culture, and the units of inheritance. *Philos Sci*. 2000; 67:S348–68. <https://doi.org/10.1086/392831>
51. Wagner DE, Klein AM. Lineage tracing meets single-cell omics: opportunities and challenges. *Nat Rev Genet*. 2020; 21:410–27. <https://doi.org/10.1038/s41576-020-0223-2> PMID: 32235876

52. Ackermann M. A functional perspective on phenotypic heterogeneity in microorganisms. *Nat Rev Micro*. 2015; 13:497–508. <https://doi.org/10.1038/nrmicro3491> PMID: 26145732
53. Waters CM, Bassler BL. Quorum sensing: cell-to-cell communication in bacteria. *Annu Rev Cell Dev Biol*. 2005; 21:319–46. <https://doi.org/10.1146/annurev.cellbio.21.012704.131001> PMID: 16212498
54. Rainey PB, Travisano M. Adaptive radiation in a heterogeneous environment. *Nature*. 1998; 394:69–72. <https://doi.org/10.1038/27900> PMID: 9665128
55. Folkesson A, Jelsbak L, Yang L, Johansen HK, Ciofu O, Høiby N, et al. Adaptation of *Pseudomonas aeruginosa* to the cystic fibrosis airway: an evolutionary perspective. *Nat Rev Microbiol*. 2012; 10:841–51. <https://doi.org/10.1038/nrmicro2907> PMID: 23147702
56. Mhatre E, Snyder DJ, Sileo E, Turner CB, Buskirk SW, Fernandez NL, et al. One gene, multiple ecological strategies: A biofilm regulator is a capacitor for sustainable diversity. *Proc Natl Acad Sci U S A*. 2020; 117:21647–57. <https://doi.org/10.1073/pnas.2008540117> PMID: 32817433
57. Spiers AJ, Kahn SG, Bohannon J, Travisano M, Rainey PB. Adaptive divergence in experimental populations of *Pseudomonas fluorescens*. I. Genetic and phenotypic bases of wrinkly spreader fitness. *Genetics*. 2002; 161:33–46. PMID: 12019221
58. Martin M, Dragoš A, Otto SB, Schäfer D, Brix S, Maróti G, et al. Cheaters shape the evolution of phenotypic heterogeneity in *Bacillus subtilis* biofilms. *ISME J*. 2020; 1–11. <https://doi.org/10.1038/s41396-020-0685-4> PMID: 32483306
59. Traverse CC, Mayo-Smith LM, Poltak SR, Cooper VS. Tangled bank of experimentally evolved *Burkholderia* biofilms reflects selection during chronic infections. *Proc Natl Acad Sci U S A*. 2013; 110: E250–9. <https://doi.org/10.1073/pnas.1207025110> PMID: 23271804
60. Winstanley C, O'Brien S, Brockhurst MA. *Pseudomonas aeruginosa* evolutionary adaptation and diversification in cystic fibrosis chronic lung infections. *Trends Microbiol*. 2016; 24:327–37. <https://doi.org/10.1016/j.tim.2016.01.008> PMID: 26946977
61. Boyd A, Chakrabarty AM. *Pseudomonas aeruginosa* biofilms: role of the alginate exopolysaccharide. *J Ind Microbiol*. 1995; 15:162–8. <https://doi.org/10.1007/BF01569821> PMID: 8519473
62. Glazier JA, Graner F. Simulation of the differential adhesion driven rearrangement of biological cells. *Phys Rev E*. 1993; 47:2128–54. <https://doi.org/10.1103/physreve.47.2128> PMID: 9960234
63. Arendt D, Musser JM, Baker CVH, Bergman A, Cepko C, Erwin DH, et al. The origin and evolution of cell types. *Nat Rev Genet*. 2016; 17:744–57. <https://doi.org/10.1038/nrg.2016.127> PMID: 27818507
64. Márquez-Zacarias P, Pineau RM, Gomez M, Veliz-Cuba A, Murrugarra D, Ratcliff WC, et al. Evolution of cellular differentiation: from hypotheses to models. *Trends Ecol Evol*. 2020; 0. <https://doi.org/10.1016/j.tree.2020.07.013> PMID: 32829916
65. Sekine R, Shibata T, Ebisuya M. Synthetic mammalian pattern formation driven by differential diffusivity of Nodal and Lefty. *Nat Commun*. 2018; 9:5456. <https://doi.org/10.1038/s41467-018-07847-x> PMID: 30575724
66. Plak K, Pots H, Haastert PJMV, Kortholt A. Direct interaction between TalinB and Rap1 is necessary for adhesion of *Dictyostelium* cells. *BMC Cell Biol*. 2016; 17:1–8. <https://doi.org/10.1186/s12860-015-0078-0> PMID: 26744136
67. Srinivasan S, Vladescu ID, Koehler SA, Wang X, Mani M, Rubinstein SM. Matrix production and sporulation in *Bacillus subtilis* biofilms localize to propagating wave fronts. *Biophys J*. 2018; 114:1490–8. <https://doi.org/10.1016/j.bpj.2018.02.002> PMID: 29590605
68. Elsholz AKW, Wacker SA, Losick R. Self-regulation of exopolysaccharide production in *Bacillus subtilis* by a tyrosine kinase. *Genes Dev*. 2014; 28:1710–20. <https://doi.org/10.1101/gad.246397.114> PMID: 25085422
69. Brückner S, Schubert R, Kraushaar T, Hartmann R, Hoffmann D, Jelli E, et al. Kin discrimination in social yeast is mediated by cell surface receptors of the Flo11 adhesin family. *elife*. 2020; 9:e55587. <https://doi.org/10.7554/eLife.55587> PMID: 32286952
70. Hirose S, Benabentos R, Ho H-I, Kuspa A, Shaulsky G. Self-recognition in social amoebae is mediated by allelic pairs of *tiger* genes. *Science*. 2011; 333:467–70. <https://doi.org/10.1126/science.1203903> PMID: 21700835
71. Mhatre E, Monterrosa RG, Kovács ÁT. From environmental signals to regulators: modulation of biofilm development in Gram-positive bacteria. *J Basic Microbiol*. 2014; 54:616–32. <https://doi.org/10.1002/jobm.201400175> PMID: 24771632
72. Lopez D, Vlamakis H, Losick R, Kolter R. Paracrine signaling in a bacterium. *Genes Dev*. 2009; 23:1631–8. <https://doi.org/10.1101/gad.1813709> PMID: 19605685

73. Lopez D, Kolter R. Extracellular signals that define distinct and coexisting cell fates in *Bacillus subtilis*. *FEMS Microbiol Rev*. 2010; 34:134–49. <https://doi.org/10.1111/j.1574-6976.2009.00199.x> PMID: 20030732
74. Rubinstein SM, Kolodkin-Gal I, Mcloon A, Chai L, Kolter R, Losick R, et al. Osmotic pressure can regulate matrix gene expression in *Bacillus subtilis*. *Mol Microbiol*. 2012; 86:426–36. <https://doi.org/10.1111/j.1365-2958.2012.08201.x> PMID: 22882172
75. Müller WEG. Origin of metazoan adhesion molecules and adhesion receptors as deduced from cDNA analyses in the marine sponge *Geodia cydonium*: a review. *Cell Tissue Res*. 1997; 289:383–95. <https://doi.org/10.1007/s004410050885> PMID: 9232818
76. Pancer Z, Kruse M, Müller I, Müller WE. On the origin of Metazoan adhesion receptors: cloning of integrin alpha subunit from the sponge *Geodia cydonium*. *Mol Biol Evol*. 1997; 14:391–8. <https://doi.org/10.1093/oxfordjournals.molbev.a025775> PMID: 9100369
77. Harwood A, Coates JC. A prehistory of cell adhesion. *Curr Opin Cell Biol*. 2004; 16:470–6. <https://doi.org/10.1016/j.ceb.2004.07.011> PMID: 15363795
78. Togashi H, Kominami K, Waseda M, Komura H, Miyoshi J, Takeichi M, et al. Nectins establish a checkerboard-like cellular pattern in the auditory epithelium. *Science*. 2011; 333:1144–7. <https://doi.org/10.1126/science.1208467> PMID: 21798896
79. Buss LW. Somatic cell parasitism and the evolution of somatic tissue compatibility. *Proc Natl Acad Sci U S A*. 1982; 79:5337–41. <https://doi.org/10.1073/pnas.79.17.5337> PMID: 6957867
80. Lakkis FG, Dellaporta SL, Buss LW. Allorecognition and chimerism in an invertebrate model organism. *Organogenesis*. 2008; 4:236–40. <https://doi.org/10.4161/org.4.4.7151> PMID: 19337403
81. Ostrowski EA, Katoh M, Shaulsky G, Queller DC, Strassmann JE. Kin discrimination increases with genetic distance in a social amoeba. *PLoS Biol*. 2008; 6:e287. <https://doi.org/10.1371/journal.pbio.0060287> PMID: 19067487
82. Lubbock R. Clone-specific cellular recognition in a sea anemone. *Proc Natl Acad Sci U S A*. 1980; 77:6667–9. <https://doi.org/10.1073/pnas.77.11.6667> PMID: 6109283
83. Cao P, Wall D. Direct visualization of a molecular handshake that governs kin recognition and tissue formation in myxobacteria. *Nat Commun*. 2019; 10:3073. <https://doi.org/10.1038/s41467-019-11108-w> PMID: 31300643
84. Honig B, Shapiro L. Adhesion protein structure, molecular affinities, and principles of cell-cell recognition. *Cell*. 2020; 181:520–35. <https://doi.org/10.1016/j.cell.2020.04.010> PMID: 32359436
85. Mukherjee S, Bassler BL. Bacterial quorum sensing in complex and dynamically changing environments. *Nat Rev Microbiol*. 2019; 17:371–82. <https://doi.org/10.1038/s41579-019-0186-5> PMID: 30944413
86. Prindle A, Liu J, Asally M, Ly S, Garcia-Ojalvo J, Süel GM. Ion channels enable electrical communication in bacterial communities. *Nature*. 2015; 527:59–63. <https://doi.org/10.1038/nature15709> PMID: 26503040
87. Pathak DT, Wei X, Dey A, Wall D. Molecular recognition by a polymorphic cell surface receptor governs cooperative behaviors in bacteria. *PLoS Genet*. 2013; 9:e1003891. <https://doi.org/10.1371/journal.pgen.1003891> PMID: 24244178
88. Rousset F, Roze D. Constraints on the origin and maintenance of genetic kin recognition. *Evolution*. 2007; 61:2320–30. <https://doi.org/10.1111/j.1558-5646.2007.00191.x> PMID: 17711465
89. Axelrod R, Hammond RA, Grafen A. Altruism via kin-selection strategies that rely on arbitrary tags with which they coevolve. *Evolution*. 2004; 58:1833–8. <https://doi.org/10.1111/j.0014-3820.2004.tb00465.x> PMID: 15446434
90. Gardner A, West SA. Social evolution: the decline and fall of genetic kin recognition. *Curr Biol*. 2007; 17:R810–2. <https://doi.org/10.1016/j.cub.2007.07.030> PMID: 17878052
91. Crozier RH. Genetic clonal recognition abilities in marine invertebrates must be maintained by selection for something else. *Evolution*. 1986; 40:1100–1. <https://doi.org/10.1111/j.1558-5646.1986.tb00578.x> PMID: 28556231
92. McDougald D, Rice SA, Barraud N, Steinberg PD, Kjelleberg S. Should we stay or should we go: mechanisms and ecological consequences for biofilm dispersal. *Nat Rev Micro*. 2012; 10:39–50. <https://doi.org/10.1038/nrmicro2695> PMID: 22120588
93. Vlamakis H, Chai Y, Beaugregard P, Losick R, Kolter R. Sticking together: building a biofilm the *Bacillus subtilis* way. *Nat Rev Micro*. 2013; 11:157–68. <https://doi.org/10.1038/nrmicro2960> PMID: 23353768
94. van Gestel J, Kolter R. When we stop thinking about microbes as cells. *J Mol Biol*. 2019; 431:2487–92. <https://doi.org/10.1016/j.jmb.2019.05.004> PMID: 31082437

95. Ansaldi M, Marolt D, Stebe T, Mandic-Mulec I, Dubnau D. Specific activation of the *Bacillus* quorum-sensing systems by isoprenylated pheromone variants. *Mol Microbiol*. 2002; 44:1561–73. <https://doi.org/10.1046/j.1365-2958.2002.02977.x> PMID: 12067344
96. Pollak S, Omer-Bendori S, Even-Tov E, Lipsman V, Bareia T, Ben-Zion I, et al. Facultative cheating supports the coexistence of diverse quorum-sensing alleles. *Proc Natl Acad Sci U S A*. 2016; 113:2152–7. <https://doi.org/10.1073/pnas.1520615113> PMID: 26787913
97. Michod RE. Cooperation and conflict in the evolution of individuality. I. Multilevel selection of the organism. *Am Nat*. 1997; 149:607–45. <https://doi.org/10.1086/286012>
98. van Gestel J, Nowak MA, Tarnita CE. The evolution of cell-to-cell communication in a sporulating bacterium. *PLoS Comput Biol*. 2012; 8:e1002818. <https://doi.org/10.1371/journal.pcbi.1002818> PMID: 23284278
99. Ispolatov I, Ackermann M, Doebeli M. Division of labour and the evolution of multicellularity. *Proc Biol Sci*. 2011;1–9. <https://doi.org/10.1098/rspb.2011.1999> PMID: 22158952
100. Michod RE. Evolution of individuality during the transition from unicellular to multicellular life. *Proc Natl Acad Sci U S A*. 2007; 104:8613–8. <https://doi.org/10.1073/pnas.0701489104> PMID: 17494748
101. Black AJ, Bourrat P, Rainey PB. Ecological scaffolding and the evolution of individuality. *Nat Ecol Evol*. 2020; 4:426–36. <https://doi.org/10.1038/s41559-019-1086-9> PMID: 32042121
102. Furusawa C, Kaneko K. Emergence of multicellular organisms with dynamic differentiation and spatial pattern. *Artif Life*. 1998; 4:79–93. <https://doi.org/10.1162/106454698568459> PMID: 9798276
103. van Gestel J, Weissing FJ. Regulatory mechanisms link phenotypic plasticity to evolvability. *Sci Rep*. 2016; 6:24524. <https://doi.org/10.1038/srep24524> PMID: 27087393
104. Duran-Nebreda S, Solé R. Emergence of multicellularity in a model of cell growth, death and aggregation under size-dependent selection. *J R Soc Interface*. 2015; 12:20140982. <https://doi.org/10.1098/rsif.2014.0982> PMID: 25551152
105. Nadell CD, Foster KR, Xavier JB. Emergence of spatial structure in cell groups and the evolution of cooperation. *PLoS Comput Biol*. 2010; 6:e1000716. <https://doi.org/10.1371/journal.pcbi.1000716> PMID: 20333237
106. Bonforti A, Duran-Nebreda S, Montañez R, Solé R. Spatial self-organization in hybrid models of multicellular adhesion. *Chaos*. 2016; 26:103113. <https://doi.org/10.1063/1.4965992> PMID: 27802680
107. Colizzi ES, Hogeweg P. High cost enhances cooperation through the interplay between evolution and self-organisation. *BMC Evol Biol*. 2016 16: 31. <https://doi.org/10.1186/s12862-016-0600-9> PMID: 26832152
108. Wakano JY, Nowak MA, Hauert C. Spatial dynamics of ecological public goods. *Proc Natl Acad Sci U S A*. 2009; 106:7910–4. <https://doi.org/10.1073/pnas.0812644106> PMID: 19416839
109. Nahum JR, Harding BN, Kerr B. Evolution of restraint in a structured rock–paper–scissors community. *Proc Natl Acad Sci U S A*. 2011; 108:10831–8. <https://doi.org/10.1073/pnas.1100296108> PMID: 21690371
110. Richard ML, Nobile CJ, Bruno VM, Mitchell AP. *Candida albicans* biofilm-defective mutants. *Eukaryot Cell*. 2005; 4:1493–502. <https://doi.org/10.1128/EC.4.8.1493-1502.2005> PMID: 16087754
111. van Gestel J, Vlamakis H, Kolter R. Division of labor in biofilms: the ecology of cell differentiation. *Microbiol Spectr*. 2015; 3: MB-0002-2014. <https://doi.org/10.1128/microbiolspec.MB-0002-2014> PMID: 26104716
112. Yan F, Yu Y, Gozzi K, Chen Y, Guo J, Chai Y. Genome-wide investigation of biofilm formation in *Bacillus cereus*. *Appl Environ Microbiol*. 2017; 83. <https://doi.org/10.1128/AEM.00561-17> PMID: 28432092
113. Noirot-Gros M-F, Forrester S, Malato G, Larsen PE, Noirot P. CRISPR interference to interrogate genes that control biofilm formation in *Pseudomonas fluorescens*. *Sci Rep*. 2019; 9:15954. <https://doi.org/10.1038/s41598-019-52400-5> PMID: 31685917
114. Shapiro JA. Bacteria as multicellular organisms. *Sci Am*. 1988; 258:82–9.
115. Shapiro JA. Thinking about bacterial populations as multicellular organisms. *Annu Rev Microbiol*. 1998; 52:81–104. <https://doi.org/10.1146/annurev.micro.52.1.81> PMID: 9891794
116. Stewart PS, Costerton JW. Antibiotic resistance of bacteria in biofilms. *Lancet*. 2001; 358:135–8. [https://doi.org/10.1016/s0140-6736\(01\)05321-1](https://doi.org/10.1016/s0140-6736(01)05321-1) PMID: 11463434
117. Webb JS, Thompson LS, James S, Charlton T, Tolker-Nielsen T, Koch B, et al. Cell death in *Pseudomonas aeruginosa* biofilm development. *J Bacteriol*. 2003; 185:4585–92. <https://doi.org/10.1128/jb.185.15.4585-4592.2003> PMID: 12867469
118. Webb JS, Givskov M, Kjelleberg S. Bacterial biofilms: prokaryotic adventures in multicellularity. *Curr Opin Microbiol*. 2003; 6:578–85. <https://doi.org/10.1016/j.mib.2003.10.014> PMID: 14662353

119. Chao L, Levin BR. Structured habitats and the evolution of anticompensator toxins in bacteria. *Proc Natl Acad Sci U S A*. 1981; 78:6324–8. <https://doi.org/10.1073/pnas.78.10.6324> PMID: 7031647
120. Kerr B, Riley MA, Feldman MW, Bohannan BJM. Local dispersal promotes biodiversity in a real-life game of rock–paper–scissors. *Nature*. 2002; 418:171–4. <https://doi.org/10.1038/nature00823> PMID: 12110887
121. Fiegna F, Yu YTN, Kadam SV, Velicer GJ. Evolution of an obligate social cheater to a superior cooper-ator. *Nature*. 2006; 441:310–4. <https://doi.org/10.1038/nature04677> PMID: 16710413
122. van Gestel J, Ackermann M, Wagner A. Microbial life cycles link global modularity in regulation to mosaic evolution. *Nat Ecol Evol*. 2019; 3:1184–96. <https://doi.org/10.1038/s41559-019-0939-6> PMID: 31332330
123. Arjes HA, Willis L, Gui H, Xiao Y, Peters J, Gross C, et al. Three-dimensional biofilm colony growth supports a mutualism involving matrix and nutrient sharing. *eLife*. 2021; 10:e64145. <https://doi.org/10.7554/eLife.64145> PMID: 33594973
124. Arnaouteli S, Bamford NC, Stanley-Wall NR, Kovács ÁT. *Bacillus subtilis* biofilm formation and social interactions. *Nat Rev Microbiol*. 2021:1–15. <https://doi.org/10.1038/s41579-021-00540-9> PMID: 33824496
125. Dragoš A, Kiese-walter H, Martin M, Hsu CY, Hartmann R, Wechsler T, et al. Division of labor during biofilm matrix production. *Curr Biol*. 2018; 28: 1903–1913.e5. <https://doi.org/10.1016/j.cub.2018.04.046> PMID: 29887307
126. D’Souza GG, Povolito VR, Keegstra JM, Stocker R, Ackermann M. Nutrient complexity triggers transi-tions between solitary and colonial growth in bacterial populations. *ISME J*. 2021:1–13. <https://doi.org/10.1038/s41396-021-00953-7> PMID: 33731836
127. Qin B, Fei C, Bridges AA, Mashruwala AA, Stone HA, Wingreen NS, et al. Cell position fates and col-lective fountain flow in bacterial biofilms revealed by light-sheet microscopy. *Science*. 2020; 369:71–7. <https://doi.org/10.1126/science.abb8501> PMID: 32527924
128. Jeckel H, Jelli E, Hartmann R, Singh PK, Mok R, Totz JF, et al. Learning the space-time phase dia-gram of bacterial swarm expansion. *Proc Natl Acad Sci U S A*. 2019; 116:1489–94. <https://doi.org/10.1073/pnas.1811722116> PMID: 30635422
129. Hartmann R, Jeckel H, Jelli E, Singh PK, Vaidya S, Bayer M, et al. Quantitative image analysis of microbial communities with BiofilmQ. *Nat Microbiol*. 2021; 6:151–6. <https://doi.org/10.1038/s41564-020-00817-4> PMID: 33398098
130. Setty M, Tadmor MD, Reich-Zeliger S, Angel O, Salame TM, Kathail P, et al. Wishbone identifies bifur-cating developmental trajectories from single-cell data. *Nat Biotechnol*. 2016; 34:637–45. <https://doi.org/10.1038/nbt.3569> PMID: 27136076
131. Haghverdi L, Büttner M, Wolf FA, Büttner F, Theis FJ. Diffusion pseudotime robustly reconstructs lineage branching. *Nat Methods*. 2016; 13:845–8. <https://doi.org/10.1038/nmeth.3971> PMID: 27571553
132. Raj B, Gagnon JA, Schier AF. Large-scale reconstruction of cell lineages using single-cell readout of transcriptomes and CRISPR–Cas9 barcodes by scGESTALT. *Nat Protoc*. 2018; 13:2685–713. <https://doi.org/10.1038/s41596-018-0058-x> PMID: 30353175
133. Nguyen Ba AN, Cvijović I, Rojas Echenique JI, Lawrence KR, Rego-Costa A, Liu X, et al. High-resolu-tion lineage tracking reveals travelling wave of adaptation in laboratory yeast. *Nature*. 2019; 575:494–9. <https://doi.org/10.1038/s41586-019-1749-3> PMID: 31723263
134. Weissman TA, Pan YA. Brainbow: new resources and emerging biological applications for multicolor genetic labeling and analysis. *Genetics*. 2015; 199:293–306. <https://doi.org/10.1534/genetics.114.172510> PMID: 25657347
135. Frieda KL, Linton JM, Hormoz S, Choi J, Chow KHK, Singer ZS, et al. Synthetic recording and *in situ* readout of lineage information in single cells. *Nature*. 2017; 541:107–11. <https://doi.org/10.1038/nature20777> PMID: 27869821
136. McDole K, Guignard L, Amat F, Berger A, Malandain G, Royer LA, et al. *In toto* imaging and recon-struction of post-implantation mouse development at the single-cell level. *Cell*. 2018; 175: 859–876. e33. <https://doi.org/10.1016/j.cell.2018.09.031> PMID: 30318151
137. Dar D, Dar N, Cai L, Newman DK. *In situ* single-cell activities of microbial populations revealed by spa-tial transcriptomics. *bioRxiv*. 2021; 2021.02.24.432792. <https://doi.org/10.1101/2021.02.24.432792>
138. Roth S. The origin of dorsoventral polarity in *Drosophila*. *Philos Trans R Soc Lond Ser B Biol Sci*. 2003; 358:1317–29. <https://doi.org/10.1098/rstb.2003.1325> PMID: 14511478
139. Roth S, Lynch JA. Symmetry breaking during *Drosophila* oogenesis. *Cold Spring Harb Perspect Biol*. 2009; 1:a001891. <https://doi.org/10.1101/cshperspect.a001891> PMID: 20066085

140. Janzen DH, Burns JM, Cong Q, Hallwachs W, Dapkey T, Manjunath R, et al. Nuclear genomes distinguish cryptic species suggested by their DNA barcodes and ecology. *Proc Natl Acad Sci U S A*. 2017; 114:8313–8. <https://doi.org/10.1073/pnas.1621504114> PMID: 28716927
141. Hebert PDN, Penton EH, Burns JM, Janzen DH, Hallwachs W. Ten species in one: DNA barcoding reveals cryptic species in the neotropical skipper butterfly *Astraptes fulgerator*. *Proc Natl Acad Sci U S A*. 2004; 101:14812–7. <https://doi.org/10.1073/pnas.0406166101> PMID: 15465915